

Sensitivity Analysis of FEMA HAZUS Earthquake Model: Case Study from King County, Washington

C. J. Neighbors¹; E. S. Cochran²; Y. Caras³; and G. R. Noriega⁴

Abstract: *Hazards U.S. Multi-Hazard Maintenance Release 4 (HAZUS-MH MR4)* is damage- and loss-estimation software developed by FEMA to estimate potential losses from natural disasters. Federal, state, regional, and local governments use the HAZUS earthquake model for earthquake risk mitigation, preparedness, response, and recovery planning. This paper examines earthquake model input parameters for earthquake source, including epicenter location, hypocentral depth, magnitude, and fault-plane dimensions, orientation, and dip, as well as geologic site conditions, to show how modifying the user-supplied settings affect ground-motion analysis, seismic risk assessment, and earthquake loss estimates. HAZUS calculates ground motion and resulting ground failure to estimate direct physical damage for general building stock, essential facilities, and lifelines, including transportation systems and utility systems. Earthquake losses in HAZUS are expressed in building-damage, economic, and social terms; this paper focuses on monetary building damages, which are predicted by building type and occupancy classification (building use). This analysis centers on both shallow crustal and deep intraslab events that affect King County, Washington, in the Pacific Northwest; however, the methods and results of this paper may help to assess the accuracy of HAZUS estimates more generally for seismically active regions. The results show that the estimated economic building damage varies by a factor of 14, on average, when using more accurate user-supplied source and site parameters rather than default values. In extreme cases, the estimated economic building damage varies by a factor of more than 500. The results also show that HAZUS scenarios for King County are more sensitive to changes in source parameters than site conditions. The considerable variability in the estimated economic building damage can have a dramatic impact on both hazard-mitigation plans and initial postevent assessments used by emergency managers. DOI: [10.1061/\(ASCE\)NH.1527-6996.0000089](https://doi.org/10.1061/(ASCE)NH.1527-6996.0000089). © 2013 American Society of Civil Engineers.

CE Database subject headings: Seismic effects; Risk management; Sensitivity analysis; Earthquakes; Case studies; Washington.

Author keywords: Seismic hazard; Risk assessment; Loss estimation; HAZUS; Sensitivity analysis; Earthquake; Modeling; Seismic effects.

Introduction to HAZUS

HAZUS is widely used loss-estimation software that provides a standardized methodology for assessing potential losses from earthquakes, floods, and hurricanes. HAZUS software operates on geographic information systems (GIS) technology to calculate potential physical, economic, and social impacts of disasters. Primary users of HAZUS, such as government officials, GIS specialists, and emergency managers and responders, use the software to develop mitigation and recovery plans as well as preparedness and response procedures for a suite of natural hazards. FEMA asserts that for state, Indian tribal, and local governments to receive non-emergency disaster assistance, the governing body must have a

standing hazard-mitigation plan (FEMA 2010). In addition to estimating losses prior to a natural hazard, governments run HAZUS scenarios after big events to estimate the degree of damage and to decide if federal recovery efforts may be needed.

Given the potential enormity of the losses associated with natural hazards, it is imperative to understand the intrinsic limitations of running natural-hazard scenarios within the HAZUS framework. Many options are available to construct an earthquake scenario within HAZUS, including input parameters describing both the earthquake source and the geologic site conditions, where manipulation of these parameters may result in widely varying outputs. Using embedded databases, such as demographic aspects of the population, building counts and construction types, and utility and transportation lines, HAZUS users can carry out general loss estimations for a study region as a result of an earthquake (Whitman et al. 1997; FEMA 2000, 2003a, b, 2008, 2010). These loss estimates are presented in terms of economic and social losses, such as calculated direct losses for buildings (occupancy class), casualties, and shelter requirements owing to damage to building stock, essential facilities, and transportation and utility systems.

Generally, model accuracy can be determined by comparison with real data; however, there have been few large earthquakes near U.S. urban centers in the last decade, yielding few rigorous tests of the HAZUS earthquake model. FEMA notes that uncertainties in the HAZUS loss-estimation model arise from incomplete scientific knowledge concerning earthquakes and their effects on buildings and facilities (FEMA 2003a). Limitations also arise from incomplete or inaccurate inventories of the built

¹Graduate Student Researcher, Dept. of Earth Sciences, Univ. of California, Riverside, CA 92521 (corresponding author). E-mail: corrie.neighbors@email.ucr.edu

²Research Geophysicist, USGS, 525 South Wilson Ave., Pasadena, CA 91106; Adjunct Professor, Dept. of Earth Sciences, Univ. of California, Riverside, CA 92521. E-mail: ecochran@usgs.gov

³Senior Geographic Information Systems (GIS) Analyst, King County GIS Center, 201 South Jackson St., Suite 706, Seattle, WA 98104. E-mail: yuko.caras@kingcounty.gov

⁴Graduate Student Researcher, Dept. of Public Health, Geologic Hazards and Disasters Research Group, Univ. of California, Irvine, CA 92697. E-mail: gnoriega@uci.edu

Note. This manuscript was submitted on May 17, 2011; approved on July 23, 2012; published online on July 26, 2012. Discussion period open until October 1, 2013; separate discussions must be submitted for individual papers. This paper is part of the *Natural Hazards Review*, Vol. 14, No. 2, May 1, 2013. ©ASCE, ISSN 1527-6988/2013/2-134-146/\$25.00.

environment, demographics, and economic parameters within the embedded database. FEMA notes that these factors can result in a range of uncertainty in loss estimates produced by the *HAZUS* earthquake model, possibly at best a factor of 2 or more (FEMA 2003b). The *HAZUS User's Manual* explicitly states that running a scenario using default data can result in incomplete estimated losses and recommends including at least some user-supplied input; however, the expected range over which the loss estimates may vary is not provided (FEMA 2003c). Al-Momani and Harrald (2003) and Kircher et al. (2006a) compared damage and loss estimated for the 1994 M_w 6.7 Northridge earthquake with actual damage and loss as a result of the earthquake and found that variations ranged between two and four for social losses (i.e., injured, killed, and displaced people). For the 1989 M_w 7.1 Loma Prieta earthquake, Al-Momani and Harrald (2003) found that social and economic losses varied within a factor of 3. Price et al. (2010) conducted a source-sensitivity study in Nevada and found that uncertainty in source characteristics can result in output variations often within a factor of 5 (i.e., total economic loss and number of buildings with major damage) but can be up to a factor of 13 (i.e., estimated fatalities).

As is inherent to any model, there are many uncertainties owing to approximations and simplifications that can have a negative impact on model results. Previous studies considered the effects of changing earthquake-source and ground-motion functions on *HAZUS* outputs, and some compared their results with measured outcomes after an earthquake (Bendimerad 2001; Comartin-Reis 2001; Al-Momani and Harrald 2003; Eguchi and Seligson 2008). To assess ground-motion accuracy in *HAZUS*, Kircher et al. (2006a) compared *HAZUS*-modeled scenarios for the 1994 Northridge earthquake and found that *HAZUS* (including site/soil amplification effects) underestimated the ground motion observed during the earthquake. Price et al. (2010) compared the impact of varying such inputs as epicenter location, hypocentral depth, magnitude, and fault-plane dip for selected cities in Nevada. Previous studies found that the variation across model scenarios depends on the *HAZUS* output examined; for example, there is more variation in estimated number of casualties than in building damage or total economic loss (Kircher et al. 2006a, b; Price et al. 2010; Shoaf and Seligson 2011). This variability has been attributed to building damage-state probabilities, such that casualties are more sensitive to the degree of damage, whereas all damage states contribute to the total economic loss (Kircher et al. 2006a).

In this study, inputs are varied for the earthquake source, such as epicenter location, hypocentral depth, magnitude, fault-plane dimensions, and fault-plane orientation and dip, as well as geologic site conditions, for seven historic earthquakes affecting King County, Washington, and examine resulting variations in peak ground acceleration (PGA) and economic building damage (EBD). While variations in some source and ground-motion parameters have been investigated and quantified by other studies (e.g., Al-Momani and Harrald 2003; Price et al. 2010), this study employs a sensitivity analysis to answer the question: How much variation in output is there between a *HAZUS* catalog or default scenario and a scenario with realistic geophysical input parameters? And more specifically, how sensitive is *HAZUS* to variations in source parameters and site inputs? The study then further explores the spatial variation in output across all scenarios to allow a better understanding of where (and, similarly, why) the variation occurs. This study aims to provide quantitative estimates of the variability in PGA and EBD owing to commonly used implementations of source and site parameters in *HAZUS* scenarios.

Introduction to the Study Region

The study area is King County, WA, which has a population of over 2 million people and is the most populated county in the state. The county includes the Seattle-Tacoma-Bellevue region, which FEMA (2008) ranks as fifth in the nation for annualized earthquake loss. The region has a high potential seismic hazard as a result of three types of earthquake events: (1) ruptures along the length of the Cascadia subduction zone capable of producing up to M_w 9 earthquakes, (2) ruptures occurring deep in the subducting oceanic slab resulting in M_w 6–7 events, and (3) ruptures along numerous shallow faults in the region (Fig. 1) (Atwater and Hemphill-Haley 1997; Goldfinger et al. 2003; Nelson et al. 2006; Bucknam et al. 1992; Atwater and Moore 1992). In the past century, this area has experienced four deep (~55 km) plate-boundary intraslab earthquake events: the 1949 M_w 6.8 Olympia, 1965 M_w 6.5 Seattle-Tacoma, 1999 M_w 5.8 Satsop, and 2001 M_w 6.8 Nisqually events. There also have been earthquakes on active shallow crustal faults within the Puget Sound area, the Mount St. Helens volcanic complex to the south, and other major fault systems in the region. In particular, the Seattle fault zone is a 4- to 7-km-wide zone of blind shallow thrust faults with slip rates estimated to be 0.7–1.1 mm/year in the Puget Sound and Seattle urban center (Danes et al. 1965; Johnson et al. 1999; Blakely et al. 2002; ten Brink et al. 2002). Because the Cascadia subduction zone earthquake is an extreme, infrequent event, the study instead focuses on historic deep intraslab events and shallow crustal earthquakes. The largest shallow crustal events to affect the region in the last three decades are the 1981 M_w 5.3 Elk Lake, the 1995 M_w 5.0 Robinson Point, and 1996 M_w 5.1 Duvall events. In total, seven historic earthquakes are analyzed to determine

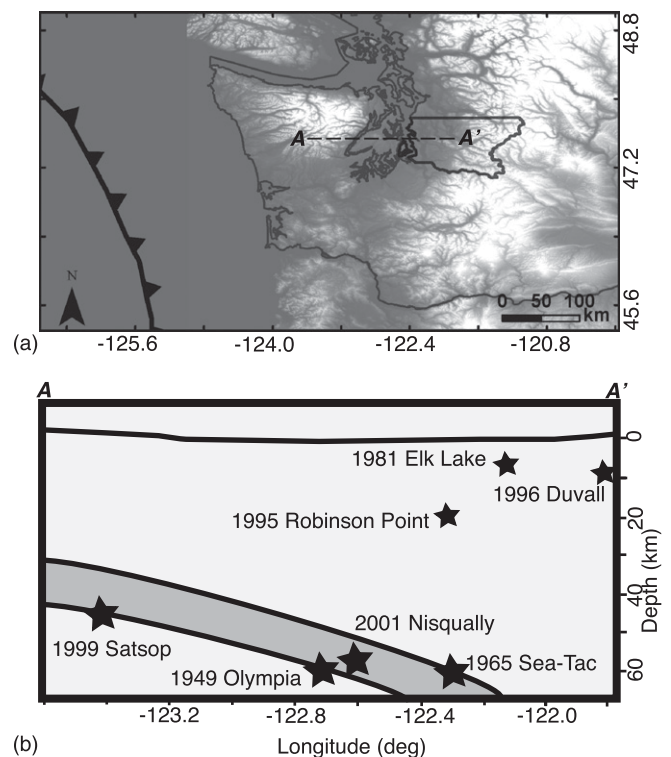


Fig. 1. (a) Tectonic setting of King County (outlined in dark gray) in Washington State relative to the Cascadia subduction zone (base map courtesy of USGS National Elevation Dataset); (b) locations of modeled earthquakes are shown as black stars on the cross-sectional schematic (deep earthquakes occur in the down-going Juan de Fuca oceanic plate, and shallow earthquakes occur in the North American continental crust)

the variability in *HAZUS* ground-motion and building-loss estimates. By constructing scenarios for seven historic earthquakes, this paper allows for a quantitative look at variation across a study region and for a better understanding of the range of *HAZUS* model results.

Ground-Motion Simulation

HAZUS Methodology

The *HAZUS* Potential Earth Science Hazards (PESH) module can be used to estimate the ground motion and resulting ground failure (i.e., liquefaction, landslide, and surface-fault rupture) from a historic earthquake source. Ground-motion estimates are functions of earthquake source, seismic wave path, and geologic site effects that contribute to the amplitude of ground shaking predicted for a given location. *HAZUS* estimates ground motions through the construction of source parameters such as fault depth, width, and length; seismic wave path through regional attenuation relationships; and soil amplification effects through National Earthquake Hazards Reduction Program (NEHRP) soil classes and amplification factors assigned to soil classes (FEMA 1997). The evaluation of ground motion is the top tier of calculations in the *HAZUS* model workflow for the purpose of calculating second-tier estimates of building damage and third-tier estimates of economic and social losses (i.e., casualties).

HAZUS generates contour maps of ground motion as well as location-specific values of ground shaking that are then used for building-damage estimates and loss calculations. Building damage is estimated using fragility curves based on the building type and response spectrum that provide the probability of damage owing to a given peak ground acceleration (PGA), peak ground displacement (PGD), or spectral demand (FEMA 2003b). The probability of damage is determined by the intersection of a building's capacity curves, or pushover displacement as a function of earthquake load, and the demand spectrum (FEMA 2003b). Because exact building specifications are rarely known at all locations, more general building inventories are often used (FEMA, 2003b). *HAZUS* calculates building damage for both structural and nonstructural components and defines four damage states from slight to complete. Building capacity curves characterizing a building's load resistance with respect to lateral displacements (ground motion) are integrated with the calculated ground motion to determine the building response. The building fragility curves are probability functions that incorporate the capacity curves, ground shaking, and building response to assign the damage states (Kircher et al. 1997a, b, 2006b; Eguchi and Seligson 2008). The resulting discrete damage states then are used to predict (1) casualties resulting from structural damage, including fatalities; (2) monetary losses resulting from building damage (i.e., cost of repairing or replacing damaged buildings and their contents); (3) monetary losses resulting from building damage and closure (e.g., losses from business interruption); (4) social impacts (e.g., loss of shelter); and (5) other economic and social impacts (FEMA 2003b). Direct economic loss from property damage is calculated as a fraction of total building exposure (i.e., total building value) and includes losses from both structural and nonstructural damage (Kircher et al. 2006a).

This study used *HAZUS-MH Maintenance Release 4* built on the platform of Environmental Systems Research Institute (ESRI) *ArcGIS 9.3.1* on the study area of King County, WA. King County was chosen because it allowed an investigation of a variety of earthquake sources (e.g., deep, shallow, normal, reverse, and strike-slip), as well as varied site effects from NEHRP soil classes ranging from B (rock) to E (soft soil). In addition, the region has experienced a sufficient number of historic earthquakes to examine in *HAZUS*. King County also has diverse demographics (indirectly related to

inventory), containing one of the 25 largest cities in the United States by population (i.e., Seattle) as well as more rural areas. As a result of this diversity, the King County region provides an ideal area to investigate the variation of *HAZUS* estimates, with results likely applicable to most seismically active regions. All models were run using the out-of-the-box population and building inventory from the U.S. Census Bureau 2000 Census data (Fig. 2). To simplify building damage estimates for the general building stock (e.g., residential, commercial, industrial, religious, government, and educational buildings), *HAZUS* aggregates the general building stock and computes the damage-state probability at the centroid of a Census tract. Using the *HAZUS* built-in U.S. Census Bureau 2000 Census data, King County has a total area of 5,896.6 km² and contains 373 Census tracts, which range in area from 0.2–1,478.1 km² (Fig. 2).

Methodology

Scenarios were constructed for the 1949 M_w 6.8 Olympia, 1965 M_w 6.6 Seattle-Tacoma, 1999 M_w 5.8 Satsop, and 2001 M_w 6.8 Nisqually deep intraslab earthquakes and the 1981 M_w 5.3 Elk Lake, 1995 M_w 5.0 Robinson Point, and 1996 M_w 5.1 Duvall shallow crustal earthquakes to examine the variation in *HAZUS* models. Three source implementations were investigated: one source supplied by the *HAZUS* historic catalog and two sources that are defined by user inputs. Each of the three source events also were run using two different types of geologic hazard parameters: *HAZUS* default inputs and user-supplied inputs for the NEHRP soil class, liquefaction susceptibility, and regional water-depth parameters. For each scenario, two *HAZUS* outputs were compared: the variation in ground motion (i.e., PGA) and economic building damage (EBD, combined structural and nonstructural damage).

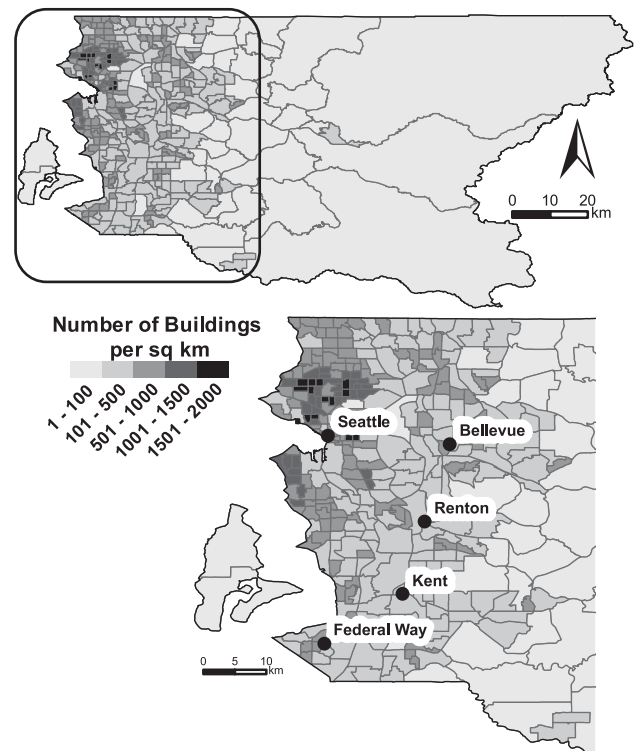


Fig. 2. Census tract boundaries and building density (number of buildings per square kilometer) for King County based on built-in *HAZUS* inventory from U.S. Census Bureau 2000 Census data: locations of five of the most populated cities are shown (solid circles)

Source-Model Input

The *HAZUS* software constructs an earthquake source using simple parameters such as epicenter location; depth; fault-plane width, orientation, and dip; and surface and subsurface rupture. Fault rupture is assumed to be of equal length on each side of the epicenter (e.g., bilateral rupture) using a finite-fault approach (FEMA 2003b; Silva et al. 2003). A parameter test was conducted to determine the range of outputs resulting from changing these basic source parameters. *HAZUS* includes a built-in earthquake catalog with source parameters for historic earthquakes developed from three sources: the Advanced National Seismic System (ANSS), the United States Geological Survey (USGS) National Earthquake Information Center (NEIC), and the National Ocean and Atmospheric Administration (NOAA) National Geophysical Data Center (FEMA 2003c). For each earthquake event, one default source from the *HAZUS* historic catalog was run, as well as two sources that were user-supplied by overriding the default parameters with characteristics unique to the earthquake (Fig. 3).

It is important to note that when a default source or an earthquake from the *HAZUS* catalog is used, a discrepancy between the catalog listing and the source input may occur. These types of discrepancies can be related to epistemic uncertainty in source characteristics, but in some cases the discrepancies are too large to be attributed to uncertainty. For example, (1) all deep events occur at 10-km depth in the *HAZUS* catalog, whereas other catalogs, including those purportedly used by *HAZUS* (FEMA 2003b), have estimated these to be 45–60 km deep (Ichinose et al. 2004, 2006; <http://www.globalcmt.org/>; <http://earthquake.usgs.gov/>); (2) all Cascadia events are given a 10-km fault width in the *HAZUS* catalog, whereas other studies estimated that fault width varies between 20 and 30 km (Ichinose et al. 2004, 2006); and (3) the 1996 Duvall shallow crustal earthquake is given a magnitude of M_w 5.8 in the default catalog but is estimated as a M_w 5.1 by the Univ. of California Berkeley Seismological Laboratory (<http://seismo.berkeley.edu/~dreger/mtindex.html>). These discrepancies are considered to be database errors in the *HAZUS* program; however, the errors were not corrected in the default-source input scenarios because a general *HAZUS* user, such as an emergency manager, may not notice or know to change these source parameters to more realistic values. For the other source implementations, a user-supplied scenario was used by inputting source parameters for the seven earthquakes based on solutions from the global centroid moment tensor (CMT) catalog (<http://www.globalcmt.org/>) and published independent studies. The first user-supplied source (Source Scenario 2-1) uses the estimated fault plane, and the second user-supplied source (Source Scenario 2-2) uses the auxiliary plane. For these two user-supplied scenarios, source parameters such as epicenter location, depth, and surface and subsurface rupture are held constant, and only the fault-plane orientation and dip are modified. It is difficult to determine which of the two fault planes given in the moment-tensor solution is the true fault without additional information; here the true fault plane was used determined by the detailed source studies of the events (Ichinose et al. 2004, 2006; Grant et al. 1984; Dewberry and Crosson 1996). However, both the true fault plane and the auxiliary plane were input to test the sensitivity of *HAZUS* to these source parameters. Input parameters for all seven earthquake sources are given in Fig. 3.

Site-Model Input

The geologic site input also was varied to compare the overall sensitivity between default and user-supplied values. *HAZUS* methodology uses site characteristics that can be input as either a singular hazard value or a mapped site-specific value to estimate loss. Some of

these site characteristics include NEHRP soil classifications and earthquake-induced landslide and liquefaction susceptibilities (Whitman et al. 1997). The NEHRP soil classes are based on the average shear-wave velocity of the upper 30 m of the geologic material. Each soil class is assigned a 0.3- and 1-s amplification factor for a given spectral acceleration (FEMA 2003b). Landslide susceptibility is estimated on a scale from 1–10 using the slope angle, critical acceleration, and geologic group. For liquefaction hazards, the probability of liquefaction occurring is a function of PGA, ground-shaking duration as reflected by earthquake magnitude, and groundwater depth. *HAZUS* uses a qualitative susceptibility rating from 0–5 (very low to very high) that is highly dependent on properties of the site geology (Youd and Perkins 1978).

Here two end-member site-scenario models characterizing geologic hazards were tested: (1) *HAZUS* default values and (2) mapped site-specific values of geologic hazards. Default values for *HAZUS-MH MR 4* are defined as NEHRP Soil Class D (stiff soil, $180 < V_s < 360$ m/s), liquefaction susceptibility rating of 0 (none), and a groundwater depth of 5 m. For the site-specific scenario, NEHRP soil classification and liquefaction susceptibility maps for King County were made available by the county as mapped by the USGS (Fig. 4). In the site-specific scenario, the default groundwater depth was adjusted from 5–17.3 m based on average water depth determined from well data provided by the county. Well data consisted of the last recorded well depth reading over the past century (1901–2005) for roughly 4,500 wells in and immediately adjacent to King County (USGS National Water Information System (<http://waterdata.usgs.gov/nwis/>)). Given the current unavailability of *HAZUS*-ready landslide susceptibility ratings for King County, this ground-failure map was not used in the analysis. In the absence of a landslide-hazard map, the landslide susceptibility rating was kept at 0 (none) for all site scenarios.

For earthquake scenarios, a user can select either a specific or a combined (dependent) attenuation relationship from those included in the *HAZUS* software based on the geographic location of the study region and, for western U.S. (WUS) studies, the faulting scenario. Attenuation describes the decrease in energy of ground shaking with increasing distance from the earthquake source. Regional geologic characteristics influence the rate at which ground motion attenuates with distance; thus users choose an attenuation function based on knowledge of the study area and source type. Previous studies found that the choice of attenuation relationship is one of the parameters that strongly influences the estimated loss (Cramer et al. 1996; Grossi 2000; Field et al. 2005). *HAZUS* allows the user to choose a specific attenuation function (Youngs et al. 1997) for a particular event scenario; however, choosing the appropriate attenuation relationship for a region requires advanced knowledge of earth science, engineering, and probabilistic methods. The default attenuation relationship in *HAZUS* is a combined attenuation relationship automatically determined based on the location of the study area (FEMA 2003b). Here the *HAZUS* combined attenuation relationships WUS Deep Event (>35 km in depth), WUS Shallow Crustal Event—Non-Extensional, and WUS Shallow Crustal Event—Extensional appropriate for each earthquake were used (FEMA 2003b).

Results

Peak Ground Acceleration and Economic Building Damage Results

For each of the seven historic earthquakes, three source scenarios and two site scenarios were modeled (total of six scenarios for each earthquake). Initially, the PGAs for each of the six scenarios were compared. PGA is computed on the default *HAZUS* contour grid of

	DEEP EVENTS			(a)	SHALLOW EVENTS			(b)
	Scenario 1	Scenario 2-1	Scenario 2-2		Scenario 1	Scenario 2-1	Scenario 2-2	
HAZUS Source Event	HAZUS Catalog Historic Event	User-supplied Event, Plane 1	User-supplied Event, Plane 2		HAZUS Catalog Historic Event	User-supplied Event, Plane 1	User-supplied Event, Plane 2	
Fault Type	Normal	Normal	Normal		Strike-Slip	Strike-Slip, R- Lateral	Strike-Slip, R- Lateral	
Attenuation Function	WUS Deep Event	WUS Deep Event	WUS Deep Event		WUS Shallow Crustal Event	WUS Shallow Crustal Event	WUS Shallow Crustal Event	
Location	47.13,-122.95 ¹	47.17,-122.62 ²	47.17,-122.62 ²		46.35,-122.24 ¹	46.76,-122.14 ⁶	46.76,-122.14 ⁶	
Magnitude	6.9 ¹	6.8 ³	6.8 ³		5.3 ¹	5.3 ⁶	5.3 ⁶	
Depth (km)	10 ¹	60 ³	60 ³		10 ¹	6.7 ⁷	6.7 ⁷	
Width (km)	10 ¹	33 ³	33 ³		10 ¹	3 ⁷	3 ⁷	
Fault Orientation (deg)	0 ¹	0 ³	43 ³		0 ¹	167 ⁶	80 ⁶	
Fault Dip (deg)	90 ¹	66 ³	31 ³		90 ¹	76 ⁶	78 ⁶	
Subsurface Length (km)	38.194 ¹	36 ³	36 ³		4.982 ¹	6 ⁷	6 ⁷	
Surface Length (km)	30.690 ¹	0.1 ¹	0.1 ¹		2.238 ¹	0.1 ¹	0.1 ¹	
Fault Type	Normal	Normal	Normal	(c)	Reverse-Slip	Reverse	Reverse	(d)
Attenuation Function	WUS Deep Event	WUS Deep Event	WUS Deep Event		WUS Shallow Crustal Event	WUS Shallow Crustal Event	WUS Shallow Crustal Event	
Location	47.40,-122.30 ¹	47.38,-122.31 ⁶	47.38,-122.31 ⁶		47.39,-122.37 ¹	47.38,-122.35 ⁸	47.38,-122.35 ⁸	
Magnitude	6.7 ¹	6.6 ⁶	6.6 ⁶		5.1 ¹	5 ⁶	5 ⁶	
Depth (km)	10 ¹	60 ⁶	60 ⁶		10 ¹	19.6 ⁸	19.6 ⁸	
Width (km)	10 ¹	20 ⁴	20 ⁴		10 ¹	1.2 ⁸	1.2 ⁸	
Fault Orientation (deg)	0 ¹	164 ⁶	64 ⁵		0 ¹	95 ⁸	136 ⁶	
Fault Dip (deg)	90 ¹	70 ⁶	24 ⁵		90 ¹	25 ⁸	58 ⁶	
Subsurface Length (km)	29.242 ¹	20 ⁴	20 ⁴		3.451 ¹	1.2 ⁸	1.2 ⁸	
Surface Length (km)	22.962 ¹	0.1 ¹	0.1 ¹		2.254 ¹	0.1 ¹	0.1 ¹	
Fault Type	Normal	Normal	Normal	(e)	Reverse-Slip	Reverse	Reverse	(f)
Attenuation Function	WUS Deep Event	WUS Deep Event	WUS Deep Event		WUS Shallow Crustal Event	WUS Shallow Crustal Event	WUS Shallow Crustal Event	
Location	47.07,-123.37 ¹	47.10,-123.43 ⁶	47.10,-123.43 ⁶		47.84,-121.74 ¹	47.82,-121.79 ⁹	47.82,-121.79 ⁹	
Magnitude	5.8 ¹	5.8 ⁶	5.8 ⁶		5.8 ¹	5.1 ⁹	5.1 ⁹	
Depth (km)	10 ¹	45 ⁶	45 ⁶		10 ¹	8 ⁹	8 ⁹	
Width (km)	10 ¹	20 ⁴	20 ⁴		10 ¹	1.3 ¹⁰	1.3 ¹⁰	
Fault Orientation (deg)	0 ¹	19 ⁶	165 ⁶		0 ¹	175 ⁹	183 ⁹	
Fault Orientation (deg)	90 ¹	34 ⁶	61 ⁶		90 ¹	52 ⁹	38 ⁹	
Fault Dip (deg)	8.790 ¹	20 ⁴	20 ⁴		8.790 ¹	1.3 ¹⁰	1.3 ¹⁰	
Surface Length (km)	6.223 ¹	0.1 ¹	0.1 ¹		6.223 ¹	0.1 ¹	0.1 ¹	
Fault Type	Normal	Normal	Normal	(g)				
Attenuation Function	WUS Deep Event	WUS Deep Event	WUS Deep Event					
Location	47.11,-122.60 ¹	47.14,-122.71 ⁴	47.14,-122.71 ⁴					
Magnitude	6.8 ¹	6.8 ⁴	6.8 ⁴					
Depth (km)	10 ¹	56 ⁴	56 ⁴					
Width (km)	10 ¹	20 ⁴	20 ⁴					
Fault Orientation (deg)	0 ¹	2 ⁶	176 ⁶					
Fault Dip (deg)	90 ¹	73 ⁶	17 ⁶					
Subsurface Length (km)	33.419 ¹	20 ⁴	20 ⁴					
Surface Length (km)	26.546 ¹	0.1 ¹	0.1 ¹					

Fig. 3. Source input parameters for the earthquake source events: (a) 1949 M_w 6.8 Olympia, (b) 1981 M_w 5.3 Elk Lake, (c) 1965 M_w 6.5 Seattle-Tacoma, (d) 1995 M_w 5.0 Robinson Point, (e) 1999 M_w 5.8 Satsop, (f) 1996 M_w 5.1 Duvall, (g) 2001 M_w 6.8 Nisqually event; Scenario 1 represents a historic event from the HAZUS earthquake catalog; Scenarios 2-1 and 2-2 are user-supplied sources using parameters from global databases and published studies [References: ¹HAZUS catalog or default HAZUS parameter; ²NEIC catalog (<http://earthquake.usgs.gov/regional/neic/>); ³Ichinose et al. 2006; ⁴Ichinose et al. 2004; ⁵Langston and Blum 1977; ⁶CMT catalog (<http://www.globalcmt.org/CMTsearch.html>); ⁷Grant et al. 1984; ⁸Dewberry and Crosson 1996; ⁹Univ. of California Berkeley Moment Tensor Solution (<http://seismo.berkeley.edu/~dreger/mtindex.html>); ¹⁰Cassidy et al. 1997]

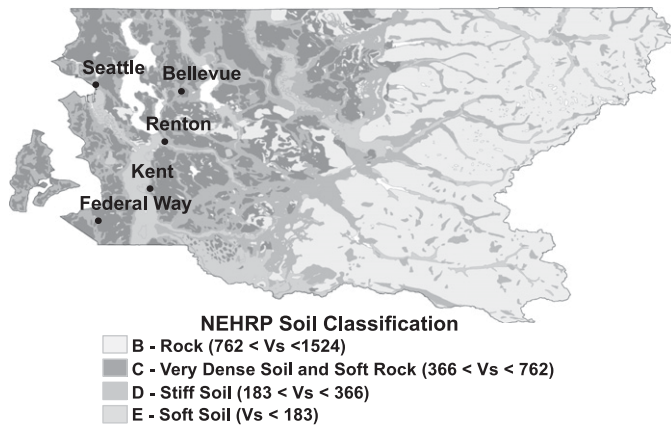


Fig. 4. NEHRP soil map for King County (USGS)

100 cells per 1° of latitude and 1° longitude, where one cell has an area of 0.85 km^2 for the King County study region. For all four deep events, the predicted PGAs are similar for each of the three source scenarios, with the two user-supplied sources producing nearly identical results for each event. The 1965 Seattle-Tacoma and 2001 Nisqually events show a clear difference in estimated PGA values between the default source and the user-supplied sources, with the default source producing higher overall ground motions (maximum $0.3\text{--}0.4g$) than the user-supplied sources (maximum $0.2\text{--}0.3g$). The event depth changes significantly between the default and user-supplied scenarios (Table 1). The depth is set to 10 km in the default catalog but increases to 60 and 56 km, respectively, in the user-supplied scenarios. Overall lower ground motion was found when a more detailed regional NEHRP soil map was used (Fig. 5). Note that this site-specific soil map has a mix of soil types, many of which have higher V_s values than the default. Using the site-specific soil map yields more spatially variable ground motions such that areas of lower V_s (soft soils E and stiff soils D) have higher and more amplified ground motions. Maps of the HAZUS-computed PGA values for the four deep earthquakes are shown in Fig. 5.

For all three shallow events, similar trends as for the deep events were found such that the two user-supplied sources produced nearly identical results for each event. The 1995 Robinson Point and 1996 Duvall earthquakes showed a clear difference in estimated PGA values between the default source and the user-supplied sources, with the default source producing higher overall ground motions (maximum $0.3\text{--}0.4g$) over larger areas. For the 1996 Duvall earthquake, these differences were most likely attributed to the change in magnitude between the default (M_w 5.8) and the user-supplied (M_w 5.1) source, as shown in Table 1. For the 1995 Robinson Point event, differences in the ground-motion maps for catalog and user-supplied scenarios may be attributed to the event depth, which is roughly doubled between the default (10 km) and user-defined (19.6 km) scenarios. Few difference in the ground motions were seen for the two user-supplied sources, which was interpreted to mean that HAZUS is not sensitive to the fault-plane orientation. Maps of the HAZUS-computed PGA values for the three shallow earthquakes are shown in Fig. 6. As with the deep events, overall lower ground motion also was found for the shallow events when using the more detailed NEHRP site-specific soil map. The peak ground motions were higher ($0.3\text{--}0.4g$) for the default site than for the site-specific soil map ($0.2\text{--}0.3g$) scenarios.

Next, the EBD values for the seven earthquake scenarios were compared (Figs. 7 and 8). The spatial patterns of EBD for the Olympia and Satsop earthquakes were similar for default and

Table 1. Variation in Economic Building Damage (EBD) in Millions of Dollars

Earthquakes	Source scenarios			Site scenarios		
	1 Default	2-1 Fault plane	2-2 Auxiliary plane	A Default	B Regional maps	
1949 M_w 6.8 Olympia factor: 3.8	0.65 – 1.78 (0.57)	0.47 – 1.31 (0.42)	0.47 – 1.31 (0.42)	1.31 – 1.78 (0.24)	0.47 – 0.65 (0.088)	
1965 M_w 6.6 Seattle-Tacoma factor: 8.3	9.47 – 13.28 (1.90)	0.74 – 0.83 (0.045)	0.75 – 0.83 (0.042)	0.74 – 9.47 (4.365)	0.83 – 13.28 (6.22)	
1999 M_w 5.8 Satsop factor ^a	0.0027 – 0.00066 (0.0010)	0.00 – 0.00063 (0.00031)	0.000016 – 0.00015 (0.000069)	0.00015 – 0.0027 (0.0013)	0.00 – 0.00066 (0.0017)	
2001 M_w 6.8 Nisqually factor: 3.3	1.97 – 2.02 (0.025)	0.61 – 1.73 (0.56)	0.65 – 1.73 (0.54)	1.73 – 1.97 (0.12)	0.61 – 2.02 (0.70)	
1981 M_w 5.3 Elk Lake factor: 130	0.00010 – 0.00054 (0.00022)	0.0039 – 0.013 (0.0046)	0.0035 – 0.012 (0.0042)	0.00054 – 0.013 (0.0063)	0.00010 – 0.0039 (0.0019)	
1995 M_w 5.0 Robinson Point factor: 5	0.24 – 0.65 (0.20)	0.14 – 0.38 (0.12)	0.13 – 0.37 (0.12)	0.37 – 0.65 (0.14)	0.13 – 0.24 (0.056)	
1996 M_w 5.1 Duvall factor: 566	0.32 – 11.31 (5.5)	0.020 – 0.064 (0.022)	0.020 – 0.065 (0.023)	0.064 – 0.32 (0.13)	0.020 – 11.31 (5.6)	

Note: The variation in EBD for a given earthquake is calculated by considering one source input while varying the site conditions or considering one site scenario while varying the source conditions. The range of variation (bold) and standard deviation are found for each scenario of a given earthquake. The factor is determined by computing the ratio between the maximum and minimum for a given earthquake. Bold = variation in building damage (millions of dollars); lightface = SD (millions of dollars).

^aFactor not computed if the EBD is 0 for any scenario.

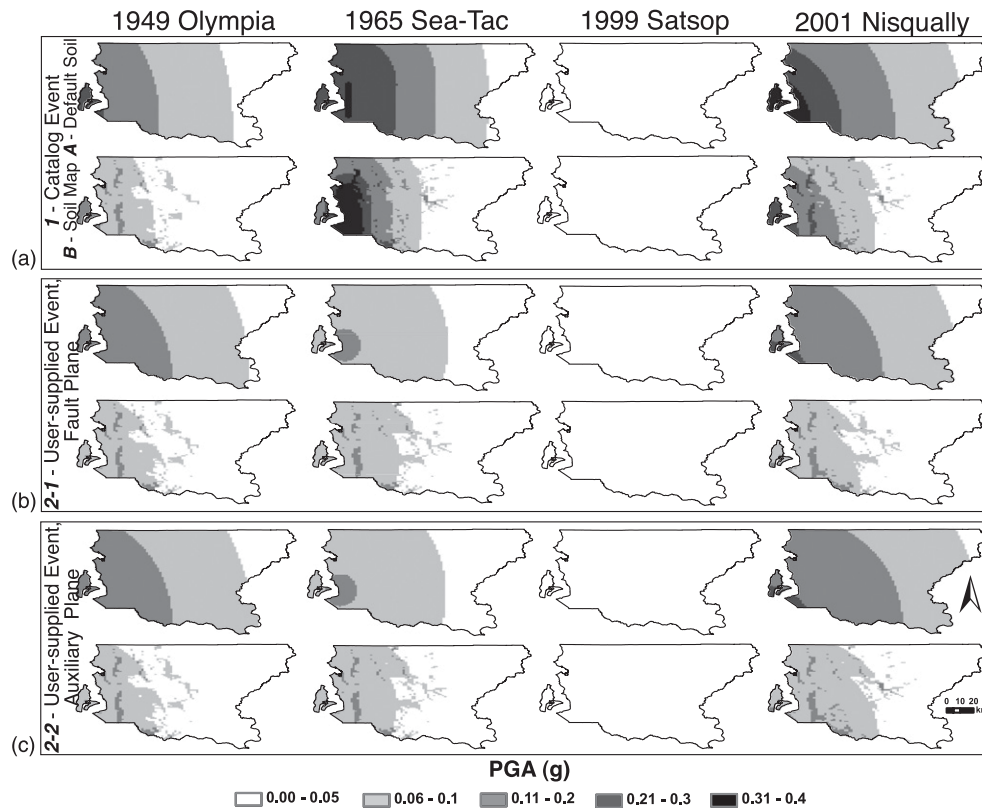


Fig. 5. Maps of PGA for the six HAZUS scenarios computed for each of the four deep earthquakes: (a) default source from HAZUS earthquake catalog; (b) and (c) user-supplied sources with preferred fault-plane orientation and auxiliary fault-plane orientation, respectively (within each part, top row represents HAZUS default-site values and bottom row represents user-supplied NEHRP site-specific soil conditions)

user-supplied sources. However, for both the 1965 Seattle-Tacoma event and the 1949 Olympia event, the default source produced slightly higher EBD values than the user-supplied scenarios, most likely because of location, magnitude, and depth differences in the source scenarios that produce higher PGAs. Interestingly, for Nisqually, damage extended across a larger area for the user-supplied source than for the default source as a result of slightly higher PGA values for the eastern Census tracts. For Seattle-Tacoma and Nisqually, there were more areas of greater damage (>\$24 million) for the default source, most likely owing to higher PGA values in the western portion of the county. For Olympia, Seattle-Tacoma, and Nisqually, EBD values were lower when the soil map was included. For the Nisqually default source scenarios, a few Census tracts using the NEHRP site-specific soil map had higher EBD values than for the default site. The 1999 Satsop event was farther from the study region and smaller in size, thus having lower values of PGA and EBD relative to the other deep events (Table 1).

The results for EBD for the three shallow earthquakes are shown in Fig. 8. Similar trends as for the shallow events were found: the two user-supplied sources produced nearly identical results for each event. However, the default source for the 1995 Robinson Point and 1996 Duvall earthquakes produced significantly higher EBD values than for the user-supplied sources. These scenarios may have higher EBD values because of differences in source parameters (i.e., magnitude and depth) between the default source scenarios and the user-supplied scenarios. Overall lower EBD values were found when the more detailed regional NEHRP soil map was used. Scenarios with the default site class had higher EBD values than the soil-map scenarios, most likely because of larger areas of high PGA.

Quantitative Comparison between Peak Ground Acceleration and Economic Building Damage

The maximum and minimum EBD values (in millions of dollars) were compared quantitatively, and the standard deviation from the average for each set of source or site scenarios was computed (Table 1). For the deep earthquakes, the largest variations were found while holding a site scenario fixed and varying the source inputs (Fig. 9). Similar results were found for the shallow earthquake events despite variable hypocenter depths and epicentral locations. For each earthquake, the ratio between the maximum and minimum EBD values also was computed for all scenario runs. For the seven earthquakes, this factor varied between 3.3 and 566, with a median value of 14.8. The factor of 566 occurs for Duvall earthquake Source Scenarios 1 and 2-2 for Site Scenario B and most likely was the result of a significant difference in the HAZUS catalog magnitude of 5.8 and the user-supplied magnitude of 5.1, in addition to other differences in source inputs, such as epicenter location and fault area and orientation.

This study also attempted to quantify the spatial variation in PGA and EBD values in order to understand where variation in the two outputs occurred across the study region. A spatial comparison of total EBD and PGA values was conducted across the six models for a single earthquake. HAZUS calculated the two outputs at different spatial resolutions, so the EBD and PGA vector data were resampled first into a uniform gridded cell raster format. For the resampled data, the cell was assigned the value of the polygon at the center of each cell. With the data in raster format, average, maximum, and minimum PGA and EBD values were determined across the county, and map algebra was used to analyze spatial

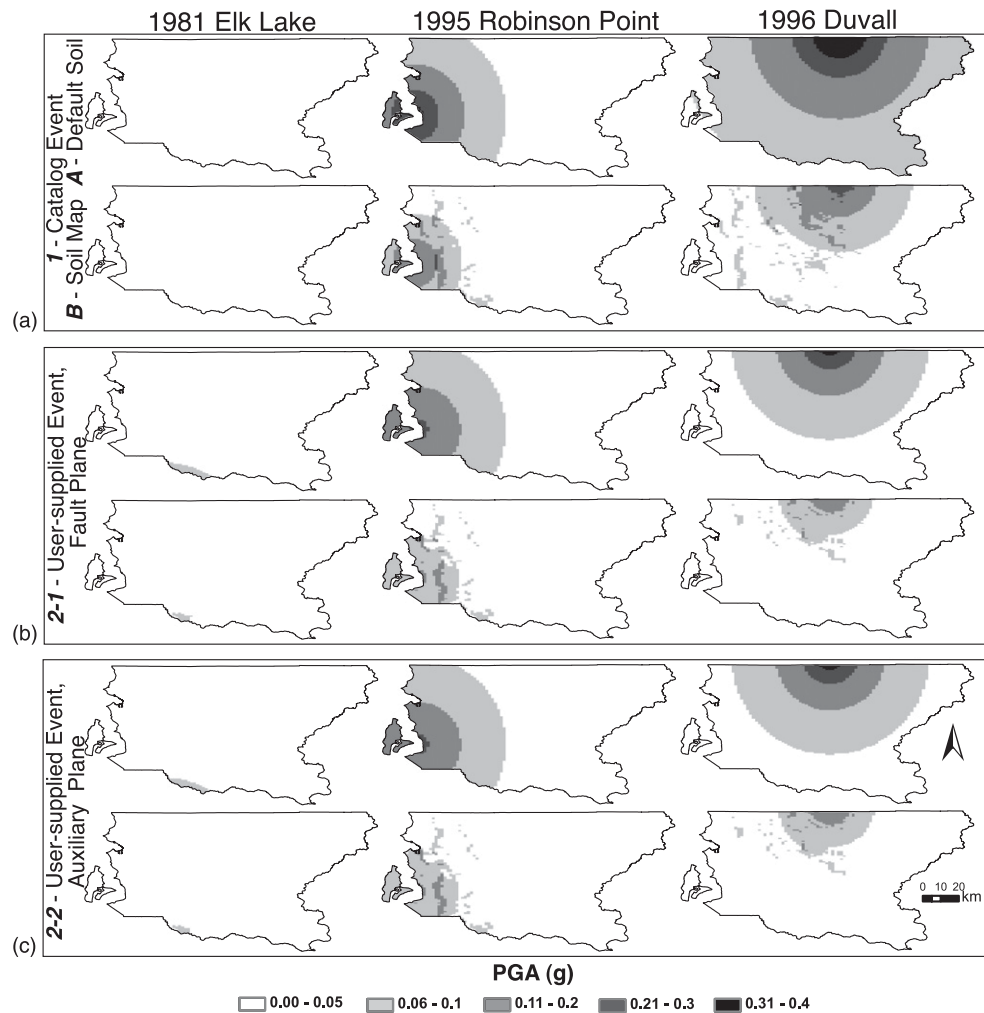


Fig. 6. Maps of PGA for the six *HAZUS* scenarios computed for each of the three shallow earthquakes: (a) default source from *HAZUS* earthquake catalog; (b) and (c) user-supplied sources with preferred fault-plane orientation and auxiliary fault-plane orientation, respectively (within each section, top row represents *HAZUS* default-site values and bottom row represents user-supplied NEHRP site-specific soil conditions)

variability in the model scenarios. Resampling was necessary prior to applying the map algebra because EBD was calculated in vector format at the center of the Census tract; Census tracts vary in area by four orders of magnitude for King County. Conversion from vector to raster format may result in positional errors and an unrealistic stepped appearance; however, these effects were minimized by upsampling to high-resolution 0.3×0.2 -km cell dimensions. For each of the six source and site scenarios, the percent difference in total EBD and PGA normalized by the average of the six scenarios run for each earthquake was calculated (Fig. 10). For each earthquake, the percent difference (here for PGA) was found by

$$\frac{\text{mean PGA}_{i,\text{single scenario}} - \text{mean PGA}_{i,\text{all scenarios}}}{\text{mean PGA}_{i,\text{all scenarios}}} \times 100\% \quad (1)$$

where i = an individual earthquake. For most scenarios, there was a clear relationship between EBD and PGA such that a scenario with higher-than-average PGA resulted in higher-than-average EBD, with the inverse relationship (lower PGA resulting in less EBD) holding true as well. However, for some scenarios, these outputs were oppositely correlated; for example, a scenario may have lower-than-average PGA but higher-than-average EBD, or vice versa. For

each scenario displaying this relationship, the normalized percentage difference in EBD and PGA was calculated on the gridded raster cells to examine the spatial correlation between the two outputs. The resulting difference maps were used to identify areas that experienced much higher- or lower-than-average PGA or EBD. Fig. 11 shows such a map for Nisqually Source Scenario 1 and Site Scenario B with an overall lower-than-average PGA (-17.5%) and higher-than-average EBD ($+31.1\%$). Exploring these outputs showed that for this earthquake scenario, PGA was lower than average for a large portion of the study region. However, PGA was higher than average in the areas of soft soil where urban centers with greater building density are located, which resulted in higher-than-average EBD. Thus, by spatially examining oppositely correlated PGA and EBD scenarios, this study highlighted the importance of including site-specific NEHRP soil maps in *HAZUS* model scenarios.

Nisqually: Comparison with ShakeMap

To determine the variation in *HAZUS* scenarios, for each event, the source and site scenarios were compared; however, it was also of interested to see how well output from scenarios created within the *HAZUS* model compared with an actual earthquake. Ideally, ground

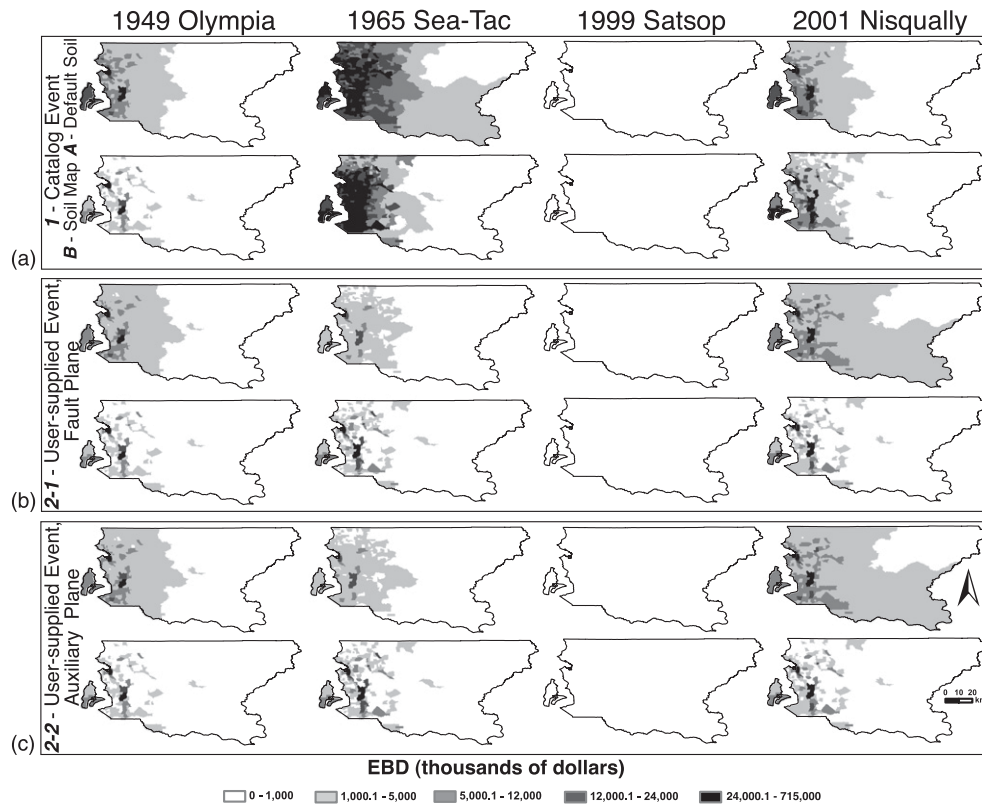


Fig. 7. Maps of EBD for the six *HAZUS* scenarios computed for each of the four deep earthquakes: (a) default source from *HAZUS* earthquake catalog; (b) and (c) user-supplied sources with preferred fault-plane orientation and auxiliary fault-plane orientation, respectively (within each section, top row represents *HAZUS* default-site values and bottom row represents user-supplied NEHRP site-specific soil conditions)

motion and damage across the county for each scenario would be compared. For the historic events model here, these data do not exist, are incomplete, or were collected at different resolutions for each event. However, prior to the 2001 Nisqually earthquake, a permanent seismic network was installed in the region that provided data to construct an interpolated USGS/PNSNxxShakeMap of ground motion for the event (Wald et al. 2005). Fig. 12 shows the USGS/Pacific Northwest Seismic Network (PNSN) ShakeMap for the 2001 M_w 6.8 Nisqually earthquake for comparison (Wald et al. 2005). By comparing the *HAZUS* scenarios for the 2001 Nisqually earthquake, it was shown that inclusion of a site map relative to the default site class (stiff soils D) produced a more realistic ground-motion map that was spatially similar to the ShakeMap of recorded ground motions, although the amplitudes of the PGAs were lower for Scenario B than the ShakeMap observed values.

Discussion and Conclusions

This study determined the variation in *HAZUS*-model-predicted PGA and EBD for both shallow crustal and deep intraslab events affecting King County. For each of the seven earthquakes, source and site inputs were varied to examine *HAZUS* sensitivity to changes in source parameters and site effects. It was found that using a default earthquake source from the *HAZUS* catalog of historic events usually produced higher PGA and EBD values than the user-supplied sources. This discrepancy is most likely the result of inaccurate default source parameters embedded within the *HAZUS* earthquake catalog, such as source depth, fault-plane dimensions, and magnitude. Given the significant database errors in the default source

catalog, *HAZUS* users are encouraged, at a minimum, to confirm source parameters using an available catalog from the USGS or another source. *HAZUS* does not appear to be sensitive to the orientation of the rupture plane if the fault does not rupture to the surface. This finding is expected considering that *HAZUS* models an earthquake as a simple bilateral rupture on a finite fault.

Whereas the conclusion here is that *HAZUS* scenarios produce large variations in output as a result of changes in source parameters between the *HAZUS* catalog and a user-supplied source, the study also found that the variation is significantly influenced by the site conditions. For local geologic hazards, it was determined that using the default singular hazard value (NEHRP Soil Class D) tends to produce higher-than-average PGA and EBD values; conversely, using a NEHRP site-specific soil and liquefaction susceptibility map produces lower-than-average PGA and EBD values. The site-specific soil map has more variability in soil type, but in particular, it includes stiff soils and bedrock (NEHRP Soil Classes B and C) that cause little to no amplification of seismic waves and therefore result in less damage to the built environment overall. It is reasonable to expect that PGA and EBD values should roughly scale such that as the PGA increases, so too should EBD. However, for some model scenarios, it was found that, for example, when PGA is lower than average, the EBD is higher than average. These oppositely correlated PGA and EBD values are attributed to the spatial distribution of PGA relative to the population centers (e.g., potential loss regions) for different scenarios. For example, in scenarios where higher-than-average ground motions (owing to soft sediments) coincided with a high-density built environment, higher-than-average property damage was found. In King County, several large cities are located on soil classes that are likely to

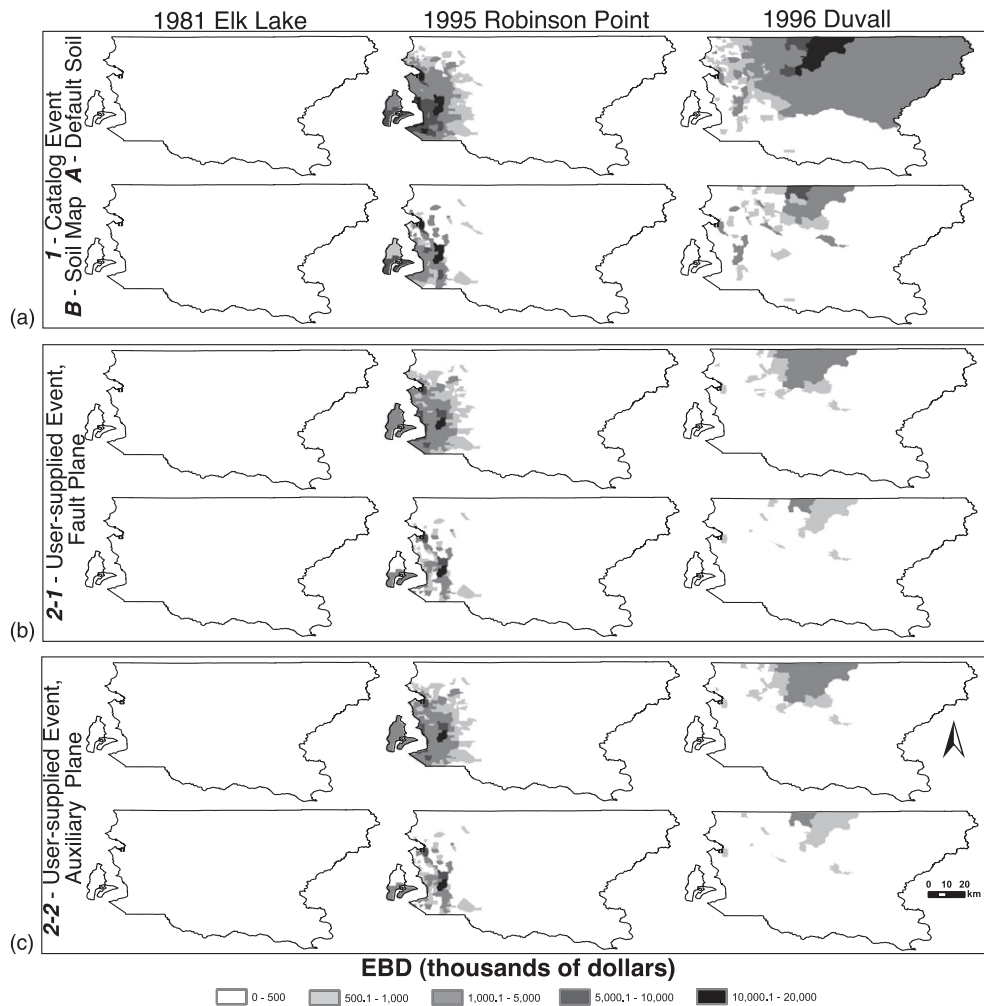


Fig. 8. Maps of EBD for the six HAZUS scenarios computed for each of the three shallow earthquakes: (a) default source from HAZUS earthquake catalog; (b) and (c) user-supplied sources with preferred fault-plane orientation and auxiliary fault-plane orientation, respectively (within each section, top row represents HAZUS default-site values and bottom row represents user-supplied NEHRP site-specific soil conditions)

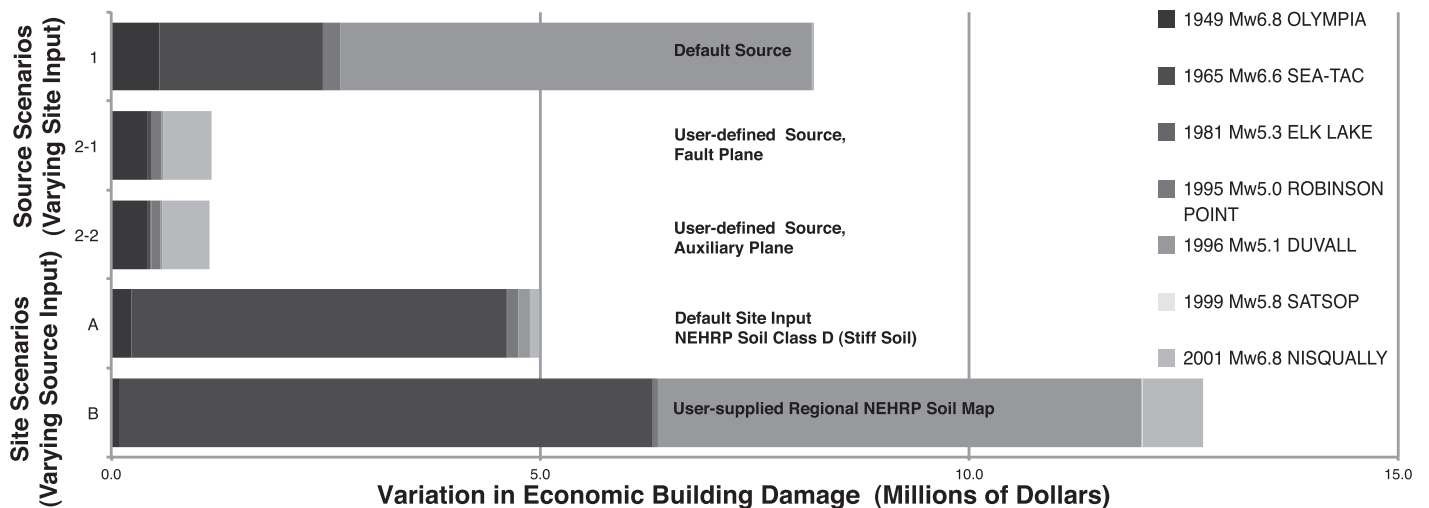


Fig. 9. Combined variation in EBD for all scenario earthquakes: top three bars represent variations caused by changing site inputs while holding the source condition constant; bottom two bars represent variation caused by changing source conditions while holding the site input constant

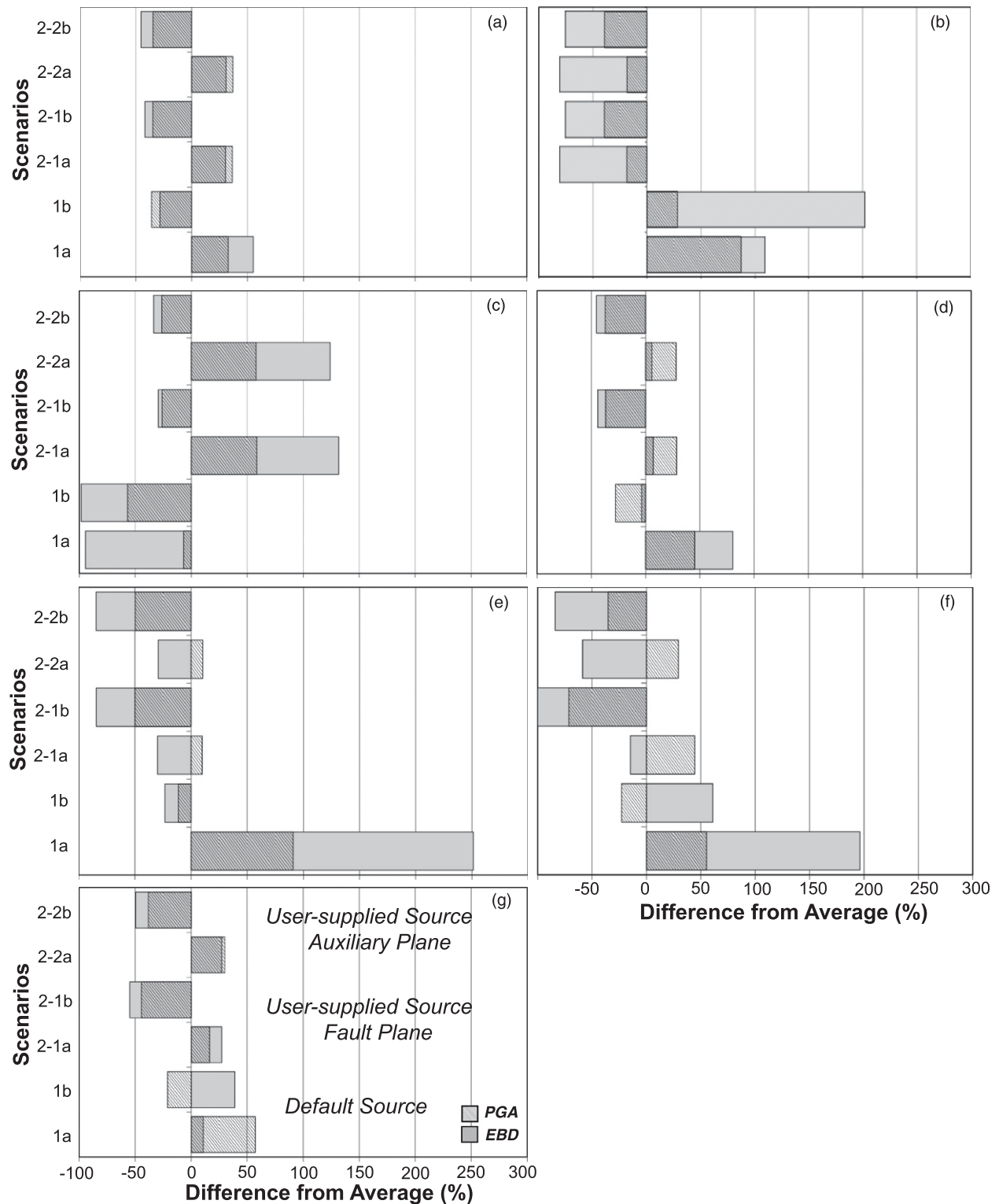


Fig. 10. Comparison of PGA and EBD for the seven historic earthquakes: (a) 1949 M_w 6.8 Olympia, (b) 1965 M_w 6.5 Seattle-Tacoma, (c) 1981 M_w 5.3 Elk Lake, (d) 1995 M_w 5.0 Robinson Point, (e) 1996 M_w 5.1 Duvall, (f) 1999 M_w 5.8 Satsop, (g) 2001 M_w 6.8 Nisqually events (plotted is the normalized difference in PGA or EBD from the average across the six source and site scenarios)

amplify ground motion, as is true for many urban areas of the United States, and thus experience greater losses. From these observations it is clear that HAZUS models should include local geologic site conditions when available. However, it is important to note that inclusion of site-specific soil maps results in computation times at least twice that of singular site values for the study region.

For the earthquake scenarios in this study, this study concludes that the user-supplied sources with user-supplied soil maps result in EBD estimates that vary by a median factor of 14. These results suggest that accurate source and site inputs are imperative to produce reasonable maps of expected PGA and EBD for hazard planning and mitigation.

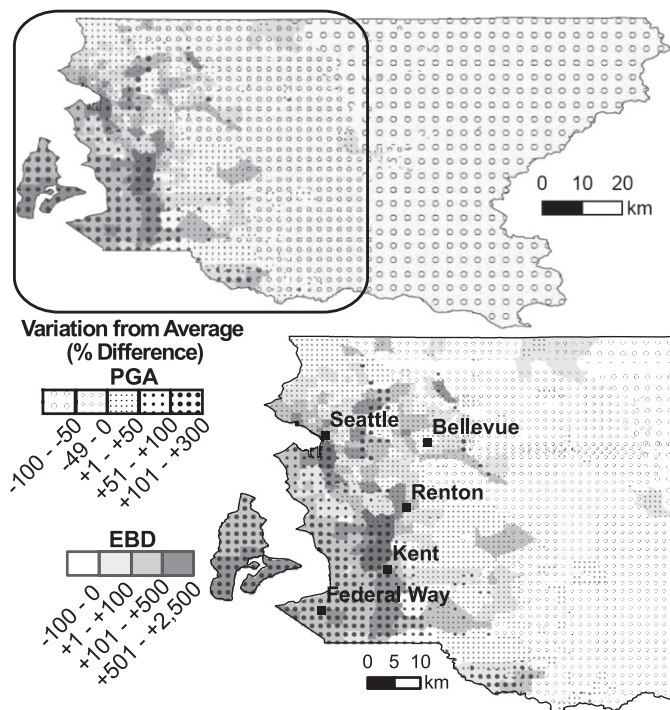


Fig. 11. Variation in PGA (open circles represent areas of lower-than-average ground motion, closed circles represent areas of higher-than-average ground motion, with the size of the circle increasing from 0% difference) and EBD (white represents areas of lower-than-average EBD and increasingly darker gray represents areas of higher-than-average EBD) for the 2001 Nisqually earthquake (shown is the PGA and EBD estimated using Source Scenario 1 and Site Scenario B conditions)

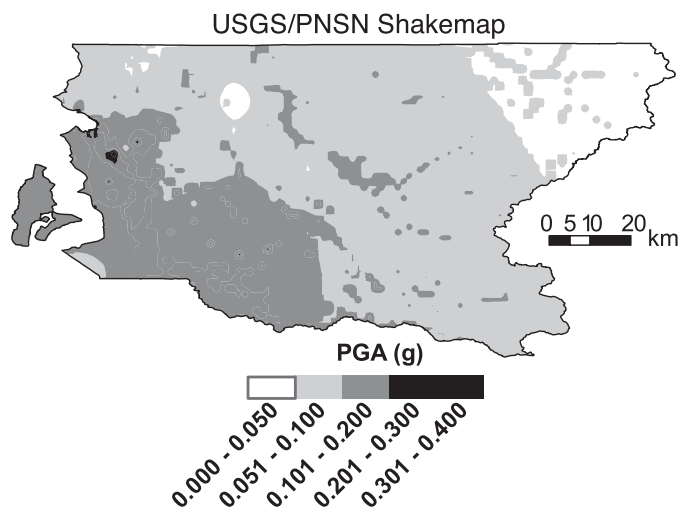


Fig. 12. USGS/PNSN ShakeMap for Nisqually earthquake showing interpolated PGA in King County

Acknowledgments

The authors thank three reviewers who provided thoughtful and detailed comments that improved the manuscript. This work greatly benefited from discussions with Hope Seligson, Phillip McCormick, and Kevin Mickey. The authors are also grateful to Washington State and King County personnel for sharing the project and

associated data, especially the staff at the Microfilm Library of the Seattle Department of Planning and Development, Gary Urbas at the Washington Emergency Management Division, and Isabelle Y. Sarikhan at the Washington Department of Natural Resources. This work was supported in part by the USGS National Earthquake Hazards Reduction Program (USGS NEHRP 2010-0019).

References

- Al-Momani, N. M., and Harrald, J. R. (2003). "Sensitivity of earthquake loss estimation model: How useful are the predictions?" *Int. J. Risk Assessment Management*, 4(1), 1–19.
- ArcGIS 9.3.1 [Computer software]. Redlands, CA, Environmental Systems Research Institute (ESRI).
- Atwater, B. F., and Hemphill-Haley, E. (1997). "Recurrence intervals for great earthquakes of the past 3500 years at northeastern Willapa Bay, Washington." *U.S. Geological Survey Professional Paper 1576*, USGS, Washington, DC, 1–108.
- Atwater, B. F., and Moore, A. L. (1992). "A tsunami about 1000 years ago in Puget Sound, Washington." *Science*, 258(5088), 1614–1617.
- Bendimerad, F. (2001). "Loss estimation: A powerful tool for risk assessment and mitigation." *Soil. Dyn. Earthq. Eng.*, 21(5), 467–472.
- Blakely, R. J., Wells, R. E., Weaver, C. S., and Johnson, S. Y. (2002). "Location, structure, and seismicity of the Seattle fault zone, Washington: Evidence from aeromagnetic anomalies, geologic mapping, and seismic reflection data." *Geol. Soc. Am. Bull.*, 114(2), 169–177.
- Bucknam, R. C., Hemphill-Haley, E., and Leopold, E. B. (1992). "Abrupt uplift within the past 1700 years at southern Puget Sound, Washington." *Science*, 258(5088), 1611–1614.
- Comartin-Reis. (2001). *HAZUS 99 SR-1 validation study*, National Institute of Building Sciences, FEMA, Washington, DC.
- Cramer, C. H., Petersen, M. D., and Reichle, M. S. (1996). "A Monte Carlo approach in estimating uncertainty for a seismic hazard assessment of Los Angeles, Ventura, and Orange counties, California." *Bull. Seismol. Soc. Am.*, 86(6), 1681–1691.
- Danes, Z. F., et al. (1965). "Geophysical investigations of the southern Puget Sound area, Washington." *J. Geophys. Res.*, 70(22), 5573–5579.
- Dewberry, S. R., and Crosson, R. S. (1996). "The M_D 5.0 earthquake of 29 January 1995 in the Puget lowland of western Washington: An event on the Seattle fault?" *Bull. Seismol. Soc. Am.*, 86(4), 1167–1172.
- Eguchi, R. T., and Seligson, H. A. (2008). "Loss estimation models and metrics." *Risk assessment, modeling and decision support, risk governance, and society*, A. Bostrom, S. French, and S. Gottlieb, eds., Vol. 14, Springer, New York, 135–170.
- FEMA. (1997). "NEHRP recommended provisions for seismic regulations for new buildings." *FEMA 302*, Washington, DC.
- FEMA. (2000). "HAZUS99 estimated annualized earthquake losses for the United States." *FEMA 366*, Washington, DC.
- FEMA. (2003a). "HAZUS99 estimated annualized earthquake losses for the United States." *FEMA 366*, Washington, DC.
- FEMA. (2003b). "HAZUS-MH MR4 technical manual, multi-hazard loss estimation methodology earthquake model." *FEMA 366*, Washington, DC.
- FEMA. (2003c). "HAZUS-MH MR4 user manual, multi-hazard loss estimation methodology earthquake model," *FEMA 366*, Washington, DC.
- FEMA. (2008). "HAZUS-MH estimated annualized earthquake losses for the United States." *FEMA 366*, Washington, DC.
- FEMA. (2010). "Hazard mitigation assistance unified guidance," *FEMA 366*, Washington, DC.
- Field, E. H., Jordan, T. H., and Cornell, C. A. (2003). "OpenSHA: A developing community-modeling environment for seismic hazard analysis." *Seismol. Res. Lett.*, 74(4), 406–419.
- Goldfinger, C., Nelson, C. H., and Johnson, J. E., Shipboard Scientific Party (2003). "Holocene earthquake records from the Cascadia subduction zone and northern San Andreas fault based on precise dating of offshore turbidites." *Annu. Rev. Earth Planet. Sci.*, 31, 555–577.

- Grant, W. C., Weaver, C. S., and Zollweg, J. E. (1984). "The 14 February 1981 Elk Lake, Washington, earthquake sequence." *Bull. Seismol. Soc. Am.*, 74(4), 1289–1309.
- Grossi, P. A. (2000). "Quantifying the uncertainty in seismic risk and loss estimation." Ph.D. thesis, Dept. of Operations and Information Management, Wharton School, Philadelphia.
- HAZUS MR4 [Computer software]. Washington, DC, FEMA.
- Ichinose, G. A., Thio, H. K., and Somerville, P. G. (2004). "Rupture process and near-source shaking of the 1965 Seattle-Tacoma and 2001 Nisqually intraslab earthquakes." *Geophys. Res. Lett.*, 31(10), L10604.
- Ichinose, G. A., Thio, H. K., and Somerville, P. G. (2006). "Moment tensor and rupture model for the 1949 Olympia, Washington, earthquake and scaling relations for Cascadia and global intraslab earthquakes." *Bull. Seismol. Soc. Am.*, 96(3), 1029–1037.
- Johnson, S. Y., Dadisman, S. V., Childs, J. R., and Stanley, W. D. (1999). "Active tectonics of the Seattle fault and central Puget Sound, Washington: Implications for earthquake hazards." *Geol. Soc. Am. Bull.*, 111(7), 1042–1053.
- Kircher, C. A., Nassar, A. A., Kustu, O., and Holmes, W. T. (1997a). "Development of building damage functions for earthquake loss estimation." *Earthq. Spectra*, 13(4), 663–682.
- Kircher, C. A., Reitherman, R. K., Whitman, R. V., and Arnold, C. (1997b). "Estimation of earthquake losses to buildings." *Earthq. Spectra*, 13(4), 703–720.
- Kircher, C. A., Seligson, H. A., Bouabid, J., and Morrow, G. C. (2006b). "When the big one strikes again—Estimated losses due to a repeat of the 1906 San Francisco earthquake." *Earthq. Spectra*, 22(S2), 297–339.
- Kircher, C. A., Whitman, R. V., and Holmes, W. T. (2006a). "HAZUS earthquake loss estimation methods." *Nat. Hazards Rev.*, 7(2), 45–59.
- Langston, C. A., and Blum, D. E. (1977). "The April 29, 1965, Puget Sound earthquake and the crustal and upper mantle structure of western Washington." *Bull. Seismol. Soc. Am.*, 67(3), 693–711.
- Nelson, A. R., Kelsey, H. M., and Witter, R. C. (2006). "Great earthquakes of variable magnitude at the Cascadia subduction zone." *Quat. Res.*, 65(2), 354–365.
- Price, J. G., et al. (2010). "Sensitivity analysis of loss-estimation modeling using uncertainties in earthquake parameters." *Environ. Eng. Geosci.*, 16(4), 357–367.
- Shoaf, K., and Seligson, H. (2011). "Estimating casualties for the southern California shakeout." Chapter 9, *Human casualties in earthquakes: Progress in modelling and mitigation*, R. Spence, E. So, and C. Scawthorn, eds., Vol. 29, Springer, Amsterdam, 125–137.
- Silva, W., Wong, I., Siegel, T., Gregor, N., Darragh, R., and Lee, R. (2003). "Ground motion and liquefaction simulation of the 1886 Charleston, South Carolina, earthquake." *Bull. Seismol. Soc. Am.*, 93(6), 2717–2736.
- ten Brink, U. S., Molzer, P. C., Fisher, M. A., Blakely, R. J., Crosson, R. S., and Creager, K. C. (2002). "Subsurface geometry and evolution of the Seattle fault zone and the Seattle basin." *Bull. Seismol. Soc. Am.*, 92(5), 1737–1753.
- Wald, D. J., Worden, B. C., Quitoriano, V., and Pankow, K. L. (2005). "ShakeMap manual: User's guide, technical manual, and software guide." *USGS Techniques and Methods 12-A1*, USGS, Washington, DC, 1–128.
- Whitman, R. V., Anagnos, T., Kircher, C. A., Lagorio, H. J., Lawson, R. S., and Schneider, P. (1997). "Development of a national earthquake loss estimation methodology." *Earthq. Spectra*, 13(4), 643–661.
- Youd, T. L., and Perkins, D. M. (1978). "Mapping of liquefaction induced ground failure potential." *J. Geotech. Eng. Div.*, 104(4), 433–446.
- Young R. R., Chiou, S. J., Silva W. L., and Humphrey J. R., (1997). "Strong ground motion attenuation relationships for subduction zone earthquakes." *Seismol. Res. Lett.*, 68(1), 58–85.